Thermo-Chemical-Mechanical Effects on Microstructure Development in Low-Alloy Steel Welds

S. S. Babu, S. A. David, and J. M. Vitek,
Oak Ridge National Laboratory, Oak Ridge, TN 37831-6096, U. S. A

Paper submitted to International Conference on
Solid-Solid Phase Transformations '99
Kyoto Park Hotel, Kyoto, Japan.

Thermo-Chemical-Mechanical Effects on Microstructure Development in Low-Alloy Steel Welds

S. S. Babu, S. A. David, and J. M. Vitek,
Oak Ridge National Laboratory, Oak Ridge, TN 37831-6096, U. S. A

Keywords: Low-Alloy Steels, δ-Ferrite, Austenite, Acicular Ferrite, Bainite, and Stress-relaxation.

Abstract

Effect of aluminum on the decomposition of δ ferrite to austenite was investigated in a low-alloy steel weld. In addition, the effect of inclusion composition on the transition from bainite to acicular ferrite during austenite decomposition was analyzed. Stress relaxation during decomposition of austenite to allotriomorphic and acicular ferrite was also characterized. Results from the above experiments illustrate the importance of thermomechanical effects on weld microstructure evolution.

Introduction

There is a growing need to describe solid to solid phase transformations in steel welds quantitatively. A fundamental understanding of these transformations would lead to the development of new steel welding consumables for wide range of applications. Phase transformations of importance include transformation of δ-ferrite to austenite and austenite to low-temperature ferrite, as well as, the reverse transformation from ferrite to austenite [1, 2]. The above transformations are influenced by thermochemical [3] and thermomechanical conditions [4] that prevail during welding. The present paper presents three case studies to illustrate the complexity of interactions between thermo, chemical and mechanical effects.

Role of chemical deoxidation conditions on the microstructural evolution

The microstructural evolution in two self-shielded flux cored arc welds was investigated. The major difference between these two welds was the concentration of residual aluminum that remains in the weld metal after the deoxidation reaction during welding. The composition of weld-1 was Fe - 0.23 C - 0.5 Mn - 1.77 Al - 0.003 Ti -0.006 O - 0.06 N (wt. %) and that of weld-2 was Fe - 0.15 C - 0.64 Mn - 0.53 Al - 0.058 Ti - 0.03 O - 0.03 N (wt. %). The weld microstructures in these two welds were different (Fig. 1).

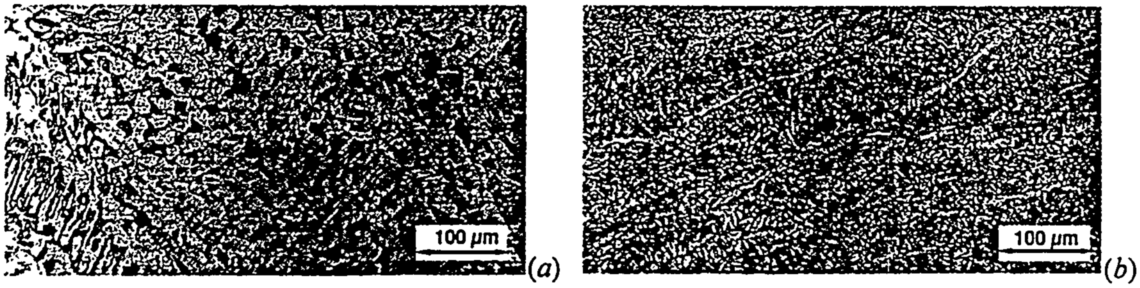

Figure 1. Optical micrograph of weld metal microstructures: (*a*) weld-1 and (*b*) weld-2.

A large concentration of aluminum in weld-1 led to a skeletal ferrite [white region in Fig. 1(*a*)] morphology and poor impact properties. This ferrite morphology was due to incomplete transformation of high-temperature δ-ferrite to austenite during weld cooling [5]. The small fraction of austenite that formed at high temperature decomposed to bainite and pearlite at lower temperatures. In contrast, weld-2 was characterized by classical ferrite morphology [see Fig. 1(*b*)] and exhibited improved impact properties. In this weld, due to a low concentration of aluminum, the transformation of δ-ferrite to austenite was complete at high temperature. On further cooling, the austenite transformed to low-temperature decomposition products such as allotriomorphic ferrite, bainite and pearlite. However, the low-aluminum concentration resulted in poor arc stability and excessive spatter. Therefore, it is important to optimize aluminum concentration in the welding consumables.

The microstructure evolution in welds is related to both concentration of aluminum as well as the cooling conditions. Specifically, the diffusion controlled growth of δ-ferrite into liquid, austenite into δ-ferrite, and austenite into liquid needs to be considered during weld cooling. In this work, the above transformations were calculated as a function of aluminum concentration with DicTra [6] software. The calculations were performed for both welds. The effect of silicon was ignored for simplicity. The calculations assumed local equilibrium at interfaces. In addition, multicomponent diffusion of Fe, C, Mn, and Al in all the phase constituents was considered. The boundary conditions for the simulations assumed a dendrite spacing of 200 μm and a linear cooling rate of 10 Ks^{-1} from 1805 K. The calculations were able to describe velocities of δ-ferrite-liquid, austenite-liquid and δ-ferrite-austenite interfaces.

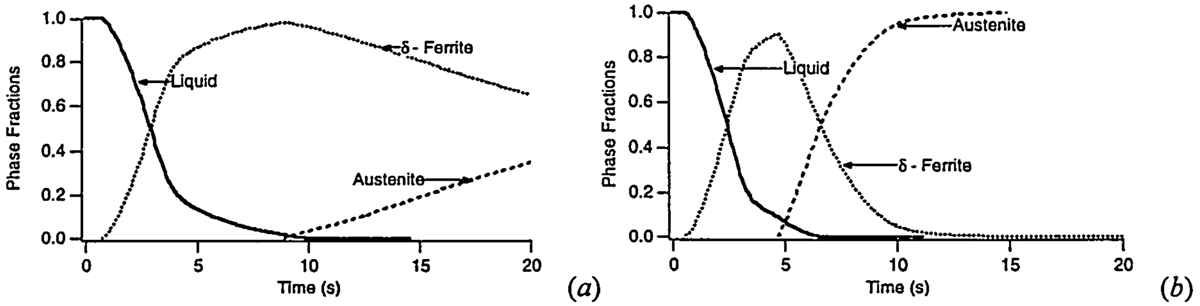

Figure 2. Predicted phase fractions for a linear cooling rate of 10 Ks^{-1}: (*a*) weld-1 and (*b*) weld-2.

The calculated phase fractions for both welds are shown in Fig. 2. The plots show [see Fig. 2(*a*)] that for high-aluminum weld 1, the solidification started with δ-ferrite formation. Later, the liquid was allowed to undergo peritectic reaction by nucleating austenite at the δ-ferrite/liquid interface and by growing into both liquid and δ-ferrite. However, transformation of δ-ferrite to austenite was not complete at 1605 K (20 s) and substantial amount of δ-ferrite was predicted to remain stable at lower temperatures. The calculations for low-aluminum weld-2 showed quite different behavior. The solidification started with the formation of δ-ferrite and the austenite formed at δ-ferrite/liquid interface. However, in contrast to weld-1, the austenite formation was complete at 1655 (15 s) K in weld-2. The results agree well with experimentally observed weld microstructure. The stability of δ-ferrite in high-aluminum weld-1 that was predicted by calculations was verified with dilatometric studies. The above result demonstrates the importance of thermochemical reaction in liquid steel on controlling the subsequent solid-state transformation.

Role of inclusions on kinetics of bainite and acicular ferrite formation

It is well known that Ti-rich inclusions promote the formation of acicular ferrite in low-alloy steel weld metals [7]. In contrast Mn- and Si-rich inclusions promote the formation of bainite for similar weld cooling conditions. In this work, the mechanism of the transition from bainite to acicular ferrite was investigated by monitoring transformation kinetics in two welds during continuous cooling. Two welds with different titanium concentrations were investigated. The composition of weld A was Fe - 0.08C - 0.32 Si - 1.58 Mn - 0.0007Ti (wt. %) and that of Weld B was Fe - 0.08 C - 0.37 Si - 1.56 Mn - 0.0032 Ti (wt. %). Weld A contained Mn- and Si- rich inclusions and Weld B Ti- rich inclusions [7]. Dilatation measurements, converted to ferrite fraction formed using standard procedures, were used to monitor the transformation kinetics during continuous cooling. The weld samples were austenitized at 1200 °C for 10 min and cooled at 50 $°Cs^{-1}$.

The microstructures and the kinetic measurements are compared in Fig. 3. Both weld samples contained small amount of grain-boundary allotriomorphic ferrite after the continuous cooling experiments. However, Weld A contained predominantly bainitic and Widmanstätten ferrite and Weld B contained acicular ferrite. This microstructural difference was similar to that found in the as-welded microstructures [7].

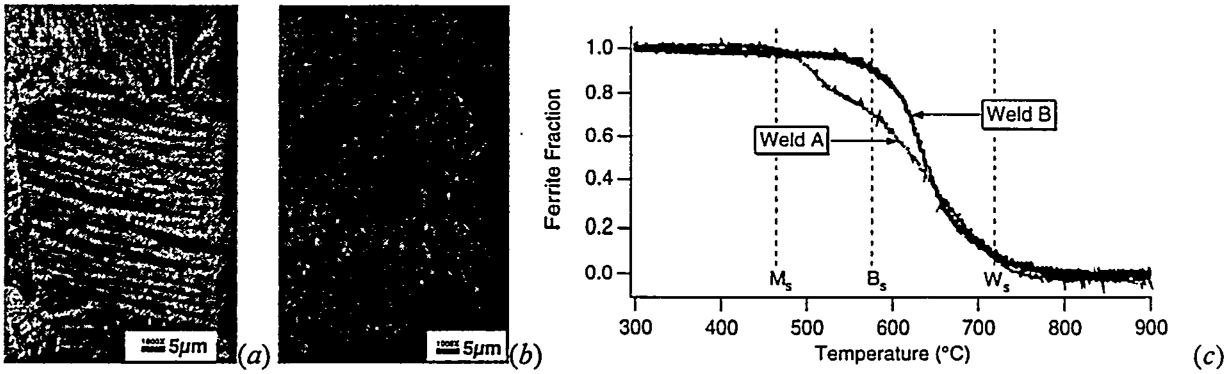

Figure 3. Microstructure of (*a*) Weld A and (*b*) Weld B after continuously cooling experiment and (*c*) measured ferrite fraction versus temperature during continuous cooling.

The measured ferrite fraction formed as a function of temperature during continuous cooling is compared in Fig. 3(*c*). The calculated Bainitic (B_s), Widmanstätten (W_s), and Martensite start (M_s) temperatures, using the method outlined in reference 8, are also shown in the figure. The plots indicate that the austenite to ferrite transformation is accelerated in Weld B compared to that of Weld A in the temperature range between W_s to B_s. The above results indicate that the Ti-rich inclusions, in addition to promoting the formation of acicular ferrite, lead to rapid transformation kinetics. Similar results were observed in other continuous cooling and isothermal transformation experiments [9]. The above results demonstrate the interactions between inclusions and the austenite to ferrite transformation kinetics [8].

Role of austenite to ferrite transformations on stress relaxation

Previous work illustrated that acicular ferrite formation interacts with an externally applied elastic stress and exhibits preferred crystallographic orientations [4]. This work suggested that transformation of austenite to different ferrite morphologies might reduce residual stresses in steel welds. To evaluate this hypothesis, stress relaxation experiments were performed on weld metal samples subjected to tensile stress while undergoing the austenite to allotriomorphic and acicular ferrite transformations. The applied load and the transformation strains (perpendicular to stress axis) were measured simultaneously in a thermomechanical simulator under isothermal conditions. The initial stress was applied by controlled straining. Transformation strains were measured in unstressed conditions also. The composition of the weld used in this experiment was Fe - 0.10 C - 0.81 Si - 1.61 Mn - 0.015 Al - 0.084 O (wt. %). The samples were austenitized at 1200 °C for 10 minutes and were quenched to the isothermal transformation temperature. For allotriomorphic ferrite, the isothermal transformation temperature was 700 °C and for acicular ferrite, it was 580 °C.

The transformation strains for the unstressed condition were expansive for both acicular ferrite and allotriomorphic ferrite formation [Fig. 4(*a*) and (*b*)]. However, under stress the acicular ferrite transformation strains showed contraction, illustrating that the transformation conforms with externally applied stress leading to transformation induced plasticity. This is in agreement with previous work [4] that shows acicular ferrite formation occurred by a displacive mechanism. However, the microstructure failed to show any obvious orientation preference of acicular ferrite platelets due to progressive reduction of stress. The transformation strains for allotriomorphic ferrite formation showed expansion, after initial contraction, illustrating the absence of compliance with stress. This is indeed expected since the allotriomorphic ferrite formation occurs by a reconstructive mechanism [8].

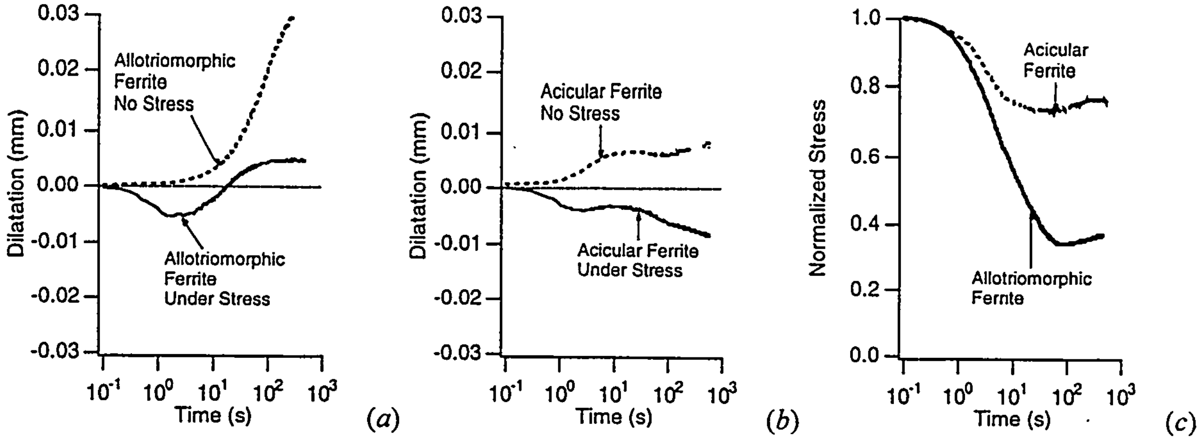

Figure 4. (*a*) Transverse transformation strains as a function of time for (*a*) allotriomorphic ferrite, (*b*) acicular ferrite and (*c*) corresponding normalized stress relaxation characteristics.

Interestingly, the measured stress relaxation results showed that the extent of stress relaxation is greater during allotriomorphic ferrite formation than during acicular ferrite formation [see Fig. 4(*c*)]. This result does not support the initial assumption that acicular ferrite formation may lead to large stress relaxation than that of allotriomorphic ferrite. Careful analysis of transformation strains in the stressed condition showed significant contraction before the initiation of allotriomorphic ferrite formation [see Fig. 4(*a*)]. This contraction is attributed to creep-relaxation of austenite at that temperature. The above work demonstrated the complex interaction between mechanical stress and the microstructure development.

Summary and conclusions

High concentration of aluminum leads to incomplete δ-ferrite to austenite transformation Fe-C-Mn-Al welds. The above phenomena can be described by diffusion controlled growth calculations. The titanium rich inclusions promoted acicular ferrite formation, as well as rapid transformation kinetics. Austenite transformation to allotriomorphic ferrite under stress leads to greater stress relaxation compared to that of acicular ferrite. All of the above results illustrate complex thermo-chemical-mechanical interactions that prevail during welding on solid to solid transformation kinetics and microstructure development.

Acknowledgement

Research sponsored by the U.S. Department of Energy, Division of Materials Sciences under contract DE-AC05-96OR22464 with Lockheed Martin Energy Research Corporation. Authors thank S. Ferree (Alloy Rods), M. Quintana (Lincoln Electric), and G. M. Evans (Oerlikon) for providing the welds.

References

1) D. J. Abson and R. J. Pargeter: Int. Met. Rev., **31**(1986), 141-194.
2) Ø. Grong and D. K. Matlock: Int. Met. Rev., **31**(1986), 27-48.
3) S. S. Babu, *et al.*: Mater. Sci. Technol., **11**(1995), 186-199.
4) S. S. Babu and H. K. D. H. Bhadeshia: Mater. Sci. Engg., **A156**(1992), 1-9.
5) M. Quintana, S. S. Babu, and S. A. David: 80th Annual AWS Convention, St. Louis, MO, 1999
6) J. Ågren: ISIJ International, **32**(1992), 291-296.
7) G. M. Evans and N. Bailey: "Metallurgy of Basic Weld Metal," Abington Publishing, England, 1997.
8) H. K. D. H. Bhadeshia, "Bainite in Steels," Institute of Materials, London, UK, 1992.
9) S. S. Babu, G. M. Evans, S. A. David: 80th annual AWS Convention, St. Louis, MO, 1999